International Journal of Mass Spectrometry 297 (2010) 28–35

Contents lists available at ScienceDirect

International Journal of Mass Spectrometry

journal homepage: www.elsevier.com/locate/ijms

Combining ion mobility mass spectrometry and infrared multiphoton dissociation spectroscopy to probe the structure of gas-phase vancomycin–$Ac_2{}^LK^DA^DA$ non-covalent complex

Jean Christophe Poully[a], Frédéric Lecomte[a], Nicolas Nieuwjaer[a], Bruno Manil[a], Jean Pierre Schermann[a], Charles Desfrançois[a], Gilles Grégoire[a,*], Renaud Ballivian[b,c,d,e], Fabien Chirot[b,c,d], Jérôme Lemoine[b,c,d], Florent Calvo[b,c,e], Rodolphe Antoine[b,c,e], Philippe Dugourd[b,c,e]

[a] *Laboratoire de Physique des Lasers, CNRS, UMR 7538, Institut Galilée, Université Paris 13, 93430, Villetaneuse, France*
[b] *Université de Lyon, F-69622, Lyon, France*
[c] *Université Lyon 1, Villeurbanne, France*
[d] *CNRS, UMR 5180, Sciences Analytiques, France*
[e] *CNRS, UMR5579, LASIM, France*

ARTICLE INFO

Article history:
Received 26 February 2010
Received in revised form 10 May 2010
Accepted 12 May 2010
Available online 20 May 2010

Keywords:
Photo action spectroscopy
Ion mobility
Mass spectrometry
Gas-phase ion structure
Molecular modeling

ABSTRACT

The structure of doubly protonated vancomycin antibiotics with its cell-wall precursor analogue $Ac_2{}^LK^DA^DA$ has been investigated in the gas phase through a combined laser spectroscopy, ion mobility and theoretical modeling approach. Replica-exchange molecular dynamics simulations using the Amber99 force field were performed to explore the potential energy landscape of isolated vancomycin ions, as well as the different binding sites with the receptor. Among the low-energy conformers found, those with a calculated diffusion cross-section consistent with ion mobility experiments were selected for further optimization, and their IR spectra were simulated using a hybrid quantum mechanics/semi-empirical (QM/SE) method at the DFT/B3LYP/6-31g(d):AM1 level. Both theoretical and experimental findings provide strong evidence that the native structure of the complex is not preserved *in vacuo* for the doubly protonated species.

1. Introduction

Infections due to Gram positive bacteria can be cured by antibiotics that target a precursor of peptidoglycans, the building blocks of the bacteria's membrane. Vancomycin (V), which is a glycopeptide, is one of these drugs. It binds strongly ($k = 1.6 \times 10^5\ M^{-1}$) to a precursor called Lipid II [1–3], which induces the cleavage of the cell-wall and eventually the death of the bacteria [4]. Early investigations have shown that the $^LK^DA^DA$ (lysine–alanine–alanine) terminal peptidic sequence of Lipid II is enantiospecifically recognized by vancomycin [5]. Resistance to vancomycin has emerged about 20 years ago with bacteria containing a mutation of the alanine terminal of this sequence into lactic acid. This mutation leads to a 1000-fold decrease in the binding affinity of the noncovalent complex, which is rationalized by the replacement of the terminal amide bond OC–NH–C of $^LK^DA^DA$ by an ester bond OC–O–C [6]. This resistance is a serious issue because vancomycin is a last-resort drug [7]. Structural studies have been carried out in the condensed phase to gain insight into the binding of vancomycin to $Ac_2{}^LK^DA^DA$ (the tripeptide is doubly protected by acetyl groups to avoid protonation and thus undesired electrostatic interactions) [8–10]. Five H-bonds tighten the two molecules, three of them involving the charged carboxylate ($CO_2{}^-$) group of the receptor and the pseudo-peptidic chain of the glycopeptide. It has been shown that the mutation of the alanine terminal sequence results in the loss of a strong hydrogen bond, which is replaced by a repulsive interaction [10,11]. A scheme of the complex in solution, with indication of the protonation and deprotonation sites, is shown in Fig. 1. Among those sites, only the receptor's carboxylate moiety is thought to play a significant role in molecular recognition [12].

In the gas phase, the absence of solvent enhances the coulombic interactions between charged groups. Therefore, the charge state is expected to impact the properties of the system. Numerous mass-spectrometric studies have been undertaken, mainly using collision-induced dissociation (CID) [13–15], but also electron capture dissociation (ECD) [16] and H/D exchange [17]. Surface-induced dissociation (SID) together with RRKM modeling has also been recently employed to probe the energetics and kinetics

* Corresponding author.
E-mail addresses: gilles.gregoire@univ-paris13.fr (G. Grégoire), fabien.chirot@adm.univ-lyon1.fr (F. Chirot), dugourd@lasim.univ-lyon1.fr (P. Dugourd).

1387-3806/$ – see front matter © 2010 Elsevier B.V. All rights reserved.
doi:10.1016/j.ijms.2010.05.014

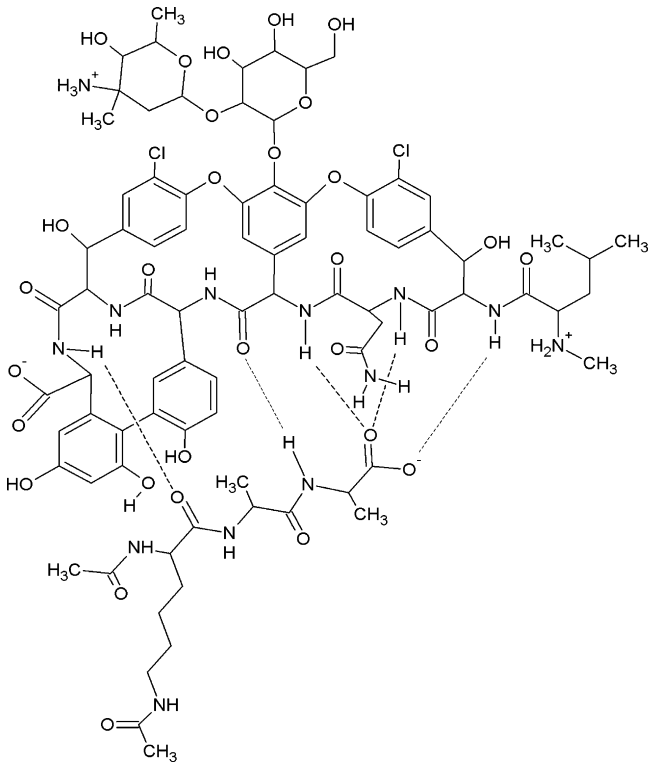

Fig. 1. Chemical structure of vancomycin (V) and the $Ac_2{}^LK^DA^DA$ peptide receptor with their most relevant hydrogen bonds (shown as dotted lines).

of vancomycin–$Ac_2{}^LK^DA^DA$ complexes [18,19]. From these studies, positively and negatively charged ions were found to adopt completely different behaviors, suggesting that conformational changes may occur upon protonation.

Some insights can be gained in the intrinsic gas-phase properties of molecular systems through IR spectroscopy. In particular, infrared multiphoton dissociation (IRMPD) is a powerful technique which allows measuring the IR spectrum of isolated systems, even without any chromophore as required for IR/UV double-resonance spectroscopy [20]. Using IRMPD, the structure of many protonated and deprotonated biologically relevant molecules at 300 K have been deciphered [21,22]. Among others, amino acids, small peptides, neurotransmitter and DNA building blocks have been studied [23–28]. However, even if IRMPD spectra of large biological systems like DNA G-quadruplexes [29] and cytochrome C [30] have been recorded, the use of quantum chemistry calculations (usually DFT methods) to interpret the IR spectra has restricted the practical size of the systems below one hundred of atoms. Besides, very few noncovalent complexes have to date been studied by IRMPD [31]. We recently proposed a methodology based on the use of a mixed quantum mechanical/semi-empirical (QM/SE) method [32], allowing the prediction of IR spectra to be extended to larger molecular systems.

Ion mobility spectrometry (IMS) is another experimental technique which can yield structural information on biomolecules. Since the pioneering works of Bowers, Jarrold and Clemmer, many studies have been undertaken on various systems, ranging from peptides [33,34] and DNA strands [35] to isolated proteins and complexes [36–42]. Such systems are much larger than those usually studied by IRMPD spectroscopy, but these two methods can complement each other if the global information on molecular shape extracted from IM is combined with the local information about intra- and inter-molecular interactions inferred from IRMPD. This dual approach, both by IMS and IR spectroscopy was recently proposed to probe the charge solvated structure of guanidiniocarbonylpyrrole-derivatives [43]. A similar dual approach has also been applied recently to study the structural properties of copper–oxytocin complexes by UV spectroscopy combined with ion mobility [44].

In the present study, the gas-phase protonated vancomycin and its complex with cell-wall precursor $Ac_2{}^LK^DA^DA$ have been investigated through the combination of IMS and IRMPD in order to probe their conformations. We focus on locating the binding site of the receptor peptide with vancomycin as a way to question whether the condensed phase structure, well known from X-ray crystallography, is preserved upon desolvation. We have recently investigated through IRMPD spectroscopy the deprotonated vancomycin complex with $Ac_2{}^LK^DA^DA$ [45]. Both theoretical and experimental findings provide strong evidence that the native structure is indeed preserved in the deprotonated complex in the gas-phase. The previous study by Roepstorff et al. [14] showed that the specific interactions between vancomycin and $Ac_2{}^LK^DA^DA$ revealed by crystallography (PDB entry 1FVM) should to be lost in the protonated ions. Our aim is thus to find out whether this loss can be explained by structural changes induced by protonation of the species.

2. Experimental

2.1. Ion mobilty spectrometry (IMS)

All IM spectra were recorded using a custom-built drift-tube coupled to a mass spectrometer. The experimental apparatus is described in more detail in other publications [44,46]. Briefly, ions are formed by electrospray ionization and transferred into RF cylindrical ion trap (CIT) through an ion funnel. The CIT is used to convert the continuous ion beam provided by the source into short (∼1 ms) ion bunches that are periodically injected into a 1 m long drift cell filled with 11.6 Torr of helium and maintained at 293 K. Ions are pulled through this cell under the influence of a weak DC electric field. Ion funnels are used to focus the diffuse ion packet at the exit of the cell and to inject it into a quadrupole time-of-flight mass spectrometer (microQTOF, Bruker). The drift time of the ions is finally recorded as a function of their mass/charge ratio. Ion mobilities and diffusion cross-sections are deduced from the arrival time distributions recorded at different drift cell voltages. In the present work, the experimental conditions were set to optimize the ion signal, leading to an IM resolution of about 35 with an uncertainty on the cross-section estimated to be less than 2%.

2.2. IRMPD spectroscopy

All IRMPD spectra have been recorded using the free electron laser (FEL) facility CLIO located at Université Paris Sud (France). The FEL laser output consists of 8 μs long macropulses at a repetition rate of 25 Hz, containing approximately 500 micropulses separated by 16 ns. The average power of the FEL is on the order of 800 mW and varies from 400 to 1000 mW over the entire spectral range. The experimental set-up has been detailed elsewhere [47]. Briefly, it consists of an electrospray ion source, an octopole guide and a Paul trap (Esquire 3000, Bruker Daltonik), in which the ions are thermalized at room temperature with a helium bath. The IR laser is sent through a hole in the ring electrode of the trap. A spectrum is recorded by scanning the laser wavenumber between 1000 and 1900 cm^{-1} and monitoring the intensity of the fragments produced upon absorption of several photons. The first absorption is resonant with the $v = 0$ to $v = 1$ transition of a vibrational mode, and the energy is redistributed by intramolecular vibrational energy redistribution (IVR) to the bath of lower-frequency modes of the ion, allowing the initially excited mode to relax to the ground state. The cycle is

repeated until the dissociation limit is reached. The intensity of the laser is adjusted to fragment a maximum of 50% of the parent ion in order to avoid saturation of the bands. The fragmentation rate is calculated as $-\ln[1 - F/(F+P)]$, where F is the sum of the fragment ions produced by IRMPD and P is the number of intact parent ions, and further normalized by the laser power [23].

The molecules were purchased from Sigma–Aldrich and used without further purification. Vancomycin and $Ac_2{}^LK^DA^DA$ were dissolved in a water/methanol solution (50/50 by volume) at equal concentrations of about 10^{-4}–10^{-5} mol/L. Injection flow rate is 150 μl/h, and we tuned the source voltages (capillary exit and entrance skimmer) in order to get the maximum signal for the non-covalent complexes.

2.3. Simulations

Structural assignments of experimental IMS and IRMPD spectra of doubly protonated vancomycin and its complex have been achieved through comparison with electronic structure calculations following conformational searches using replica-exchange molecular dynamics (REMD) simulations [48]. These simulations used the Amber 99 force field [49], and were conducted using 30 replicas with a geometric progression in temperature in the range 100–1000 K. Each trajectory used a time step of 1 fs and was propagated for 1 ns, thermostatting being achieved using a Berendsen thermostat with a coupling constant of 1 ps^{-1}. Random exchanges between adjacent pairs of replicas were attempted every 100 fs. The simulations also included a first thermalization stage of 20 ps, after which instantaneous structures were saved every 20 ps for each replica. About 1500 structures were thus obtained and locally optimized by conjugate gradient. For the lowest energy conformers, a clustering process (with the XCluster program [50] from Schrödinger INC) was used to obtain the main structural families. Here a family is defined by a common global conformation, differences between members originating from minor details such as rotations of aliphatic amino acid side chains. For each of these families, a reoptimization of the lowest energy conformer was carried out at the AM1 level. Finally, the diffusion cross-section for each conformer was calculated using the direct trajectory method [51]. Further structural optimization before this last calculation step was not needed since only minor variations of the diffusion cross-section were found to occur.

Since IR simulations by electronic structure methods are much more involved than cross-section calculations, we excluded the families of conformers whose calculated cross-sections did not agree with the IM data. For each family, the IR spectra of the lowest energy conformers were simulated with a combined quantum mechanical/semi-empirical (QM/SE) method, using the ONIOM program implemented in the Gaussian 09 package [52]. Vancomycin and its complexes contain more than 175 atoms, and DFT/B3LYP/6-31g(d) calculations are unaffordable. We thus chose to use the ONIOM method to predict the harmonic frequencies. Our methodology has been described in detail in a recent publication where we evaluated and validated this method for the prediction of IR spectra of biologically relevant molecules [32]. The system is divided into a high layer (HL) and a low layer (LL), treated at the DFT/B3LYP/6-31g(d) and AM1 levels, respectively. This combination has been found to be a good trade-off for the prediction of normal vibrational mode frequencies. However, frequencies of the atoms within the LL being described by the less reliable AM1 method, we kept only those of the HL for simulating the IR spectrum. In vancomycin and its complexes with $Ac_2{}^LK^DA^DA$, the major IR absorbing groups (COH, amide bonds, $NH_3{}^+$, NH_2, CO_2H, COC) are spread all over the system. Since all the atoms must be included in the HL to correctly simulate the IR spectrum, several calculations are needed to obtain the whole spectrum. For instance, vancomycin

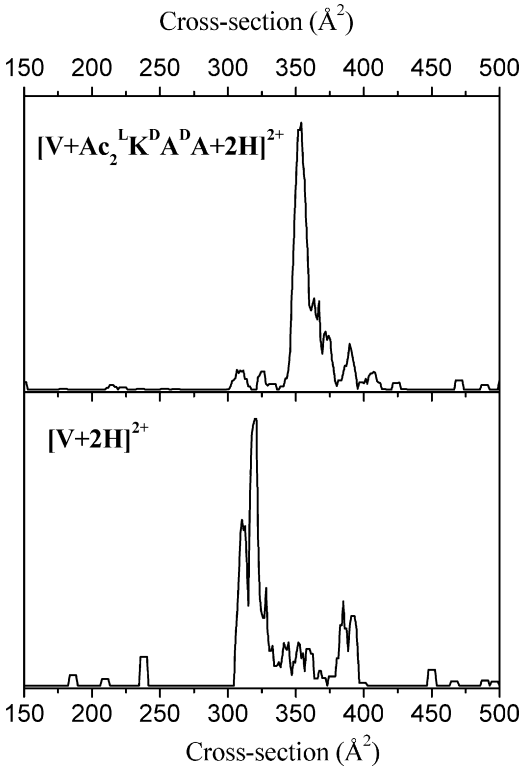

Fig. 2. Ion mobility spectra (diffusion cross-section in Å²) of $[V+2H]^{2+}$ (bottom) and $[V+Ac_2{}^LK^DA^DA+2H]^{2+}$ (top).

ions need two of them, one for the three substituted aromatic groups and the disaccharide moiety attached to it, and one for the complementary part including the pseudo-peptidic chain and the phenolic groups (*cf.* Fig. S1 of the Electronic Supplementary Information (ESI)). The two optimized structures must be very similar, that is, their minimum root mean-square deviation (RMSD) must be as small as possible. This condition was fulfilled for all the conformers considered, with RMSD not exceeding 1.2 Å. Regarding the complex, a crucial point is that we also describe the vancomycin atoms H-bound to the receptor at the DFT/B3LYP level, in order to correctly reproduce the spectral shifts induced by the intermolecular interactions. The DFT frequencies were then scaled by specific ONIOM factors (determined in our previous work [32]) for C=O stretching (0.957), NH (0.964) and NH_2 (0.964) bending modes, and by the NIST factor for the B3LYP/6-31g(d) level of theory (0.960) for the other modes [53]. The theoretical scaled frequencies were then convoluted by a Gaussian function (width of 25 cm^{-1}) accounting for the finite width of the laser (*ca.* 10 cm^{-1}) and for some rotational broadening at 300 K.

3. Experimental results

The distribution of diffusion cross-sections measured for $[V+2H]^{2+}$ and $[V+Ac_2{}^LK^DA^DA+2H]^{2+}$ is reported in Fig. 2. They are both dominated by one main peak centered at 318 and 355 Å², respectively, with ~10 Å² FWHM. The width of this peak is consistent with the diffusion of a single conformer [54]. In the distribution for vancomycin, a second peak of lower intensity is observed around 390 Å². We show in the next section from conformational searches that $[V+2H]^{2+}$ is rather rigid and cannot unfold to reach such a high cross-sections. However, it is important to note that all measurements have been made by injecting a single solution containing both vancomycin and $Ac_2{}^LK^DA^DA$, the contribution of each species being straightforwardly separated owing to the mass dif-

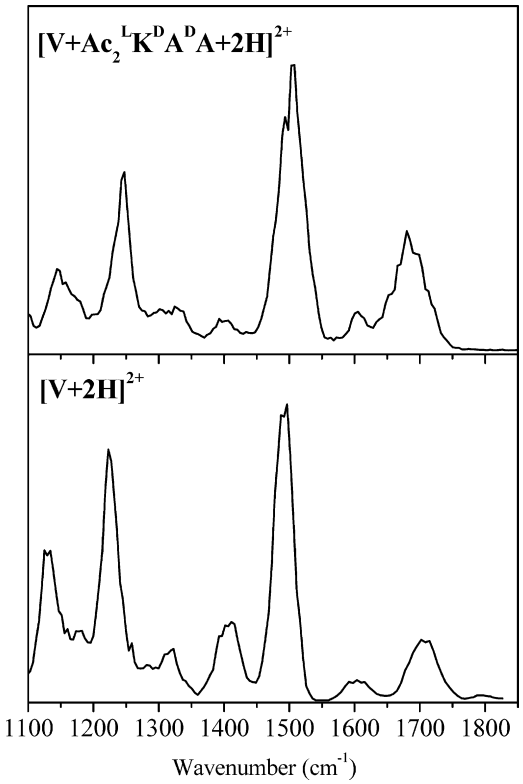

Fig. 3. IRMPD spectra of $[V+2H]^{2+}$ (bottom) and $[V+Ac_2{}^{L}K^{D}A^{D}A+2H]^{2+}$ (top).

ference. As a consequence, if fragmentation occurs in the ion optics between the end of the drift-tube and the extraction region of the time-of-flight mass spectrometer, signal is recorded for the fragment mass and parent drift time. This may explain the presence of the peak at 390 Å^2 in the spectrum recorded for vancomycin, which may correspond to a loosely bound complex whose fragmentation yields $[V+2H]^{2+}$. Under this hypothesis, the only signal attributed to the diffusion of $[V+2H]^{2+}$ is the most intense peak at 318 Å^2, and the diffusion cross-section of the complex is found to be 11% larger than the one for bare vancomycin ion.

The fragmentation pathways observed upon IRMPD of $[V+2H]^{2+}$ and $[V+Ac_2{}^{L}K^{D}A^{D}A+2H]^{2+}$ are similar to those previously found in surface- and collision-induced dissociation experiments [15,18,19]. For instance, the doubly protonated complex dissociates into singly protonated vancomycin and receptor ions. The IRMPD spectra are reported in Fig. 3. The first remarkable property is the rather low bandwidths of typically 30–40 cm^{-1}, which is comparable to those obtained for much smaller species. This value has been found to be mainly due to the intrinsic width of the FEL and to rotational broadening at 300 K. Besides, much attention has been paid to avoid saturation effect by adjusting the irradiation time and the FEL intensity with optical attenuators (reducing the main power by a factor of 3 or 6 in the case of the binary complex). In addition, the cyclic structure of vancomycin might prevent a large conformational heterogeneity, which is consistent with the narrow peaks compatible with the diffusion of a single conformer of the ion mobility spectra. The most intense IRMPD bands are attributed to the Amide I and II bands located around 1700 and 1500 cm^{-1}, as well as to C–O–H bending and C–O–C stretching modes around 1150 and 1225 cm^{-1}, respectively. Other weak transitions lying at 1600 and 1400 cm^{-1} are assigned to deformation modes of the aromatic rings. The effects of complexation are clearly visible in Fig. 3 by comparing the IR spectra of the doubly protonated vancomycin to its complex. In the complex, the Amide I band is broadened (from 40 to 54 cm^{-1}) and shifted to the red (−25 cm^{-1}) while the Amide II band is slightly broadened and shifted to the blue (+10 cm^{-1}). These spectral shifts are related to the involvement of carbonyl and amide groups of vancomycin and/or the receptor in hydrogen bonding. In addition, the bands due to the absorption of the disaccharide group (C–O–H bending and C–O–C stretching modes) are also slightly blue-shifted (+10 cm^{-1}) in the complex, which might suggest that the sugar moiety also interacts with the receptor.

4. Discussion

The first issue to be addressed is related to the protonation site in vancomycin and its complex. Vancomycin has two strong basic sites at the methylated N-terminal and at the disaccharide amine groups, consistent with the doubly protonated species detected in the mass spectrum. Besides, ECD experiments carried out by Haselmann et al. on $[V+2H]^{2+}$ lead to the appearance of fragments corresponding to the methylated N-terminus and the disaccharide moiety [16]. Therefore, these groups are probably protonated. In the $V–Ac_2{}^{L}K^{D}A^{D}A$ complex, acetylation of the N-terminus and the lysine side chain is expected to prevent the receptor from being protonated, although a small signal at the mass of the protonated $Ac_2{}^{L}K^{D}A^{D}A$ is detected. It is thus tempting to assume that vancomycin has the same protonation state in the complex as in the isolated molecule, which would imply that the receptor is neutral. It is worth mentioning that SID, CID and IRMPD of $[V+Ac_2{}^{L}K^{D}A^{D}A+2H]^{2+}$ produce mainly $[V+H]^{+}$ and $[Ac_2{}^{L}K^{D}A^{D}A+H]^{+}$ fragments. Nevertheless, proton transfer from doubly protonated vancomycin to neutral $Ac_2{}^{L}K^{D}A^{D}A$ after slow activation may occur: this may be the case in $[K_5+CD+2H]^{2+}$ complexes, where CD stands for cyclodextrin, a cyclic saccharide molecule without any strongly basic site in solution. K_5 is certainly doubly protonated in the complex, but CID leads to $[K_5+H]^{+}$ and $[CD+H]^{+}$ [55].

An interesting issue is to determine whether the condensed phase structure is preserved in the gas-phase. From the REMD simulation on $[V+Ac_2{}^{L}K^{D}A^{D}A+2H]^{2+}$, we found that among the 1180 different conformers found, only three contain a receptor located in the binding pocket of vancomycin. In addition, these conformers lie 96, 112 and 125 kJ/mol higher than the lowest energy structure (at the Amber99 level). Consequently, the native interactions revealed by X-ray and NMR measurements do not seem to be favored. In addition, the calculated diffusion cross-section of the PDB conformer after optimization at the AM1 level is 370 Å^2. Considering the position of the experimental main peak and the precision of the experiment (355 ± 4 Å^2), the crystallographic structure can be excluded by our mobility measurements. Furthermore, the Amide I band in the simulated spectrum at the ONIOM DFT/B3LYP/6-31g(d):AM1 level does not agree with the experimental spectrum (see ESI Fig. S2). We also considered the PDB conformer of $[V+2H]^{2+}$. The calculated diffusion cross-section after optimization at the AM1 level is 334 Å^2, which is clearly higher than the main mobility peak located at 318 Å^2. This conformer has a fairly extended structure, and vancomycin cannot unfold much more due to its high rigidity, which gives support to our hypothesis that the mobility peak around 390 Å^2 cannot be due to real structures of vancomycin ions. Besides, the Amide I band in the simulated IR spectrum at the ONIOM DFT/B3LYP/6-31g(d):AM1 level (ESI Fig. S2) is strongly red-shifted (40 cm^{-1}) with respect to the IRMPD spectrum.

As native vancomycin and vancomycin-receptor structures do not seem to be preserved in the gas-phase, REMD simulations were carried out to investigate the possible structures of the doubly protonated species. First, we consider the isolated glycopeptide. A preliminary study based on conformational sampling of the torsional degrees of freedom [32] revealed three main families of conformers, denoted below as V_1, V_2 and V_3. A more complete investigation was carried out by clustering the lowest energy con-

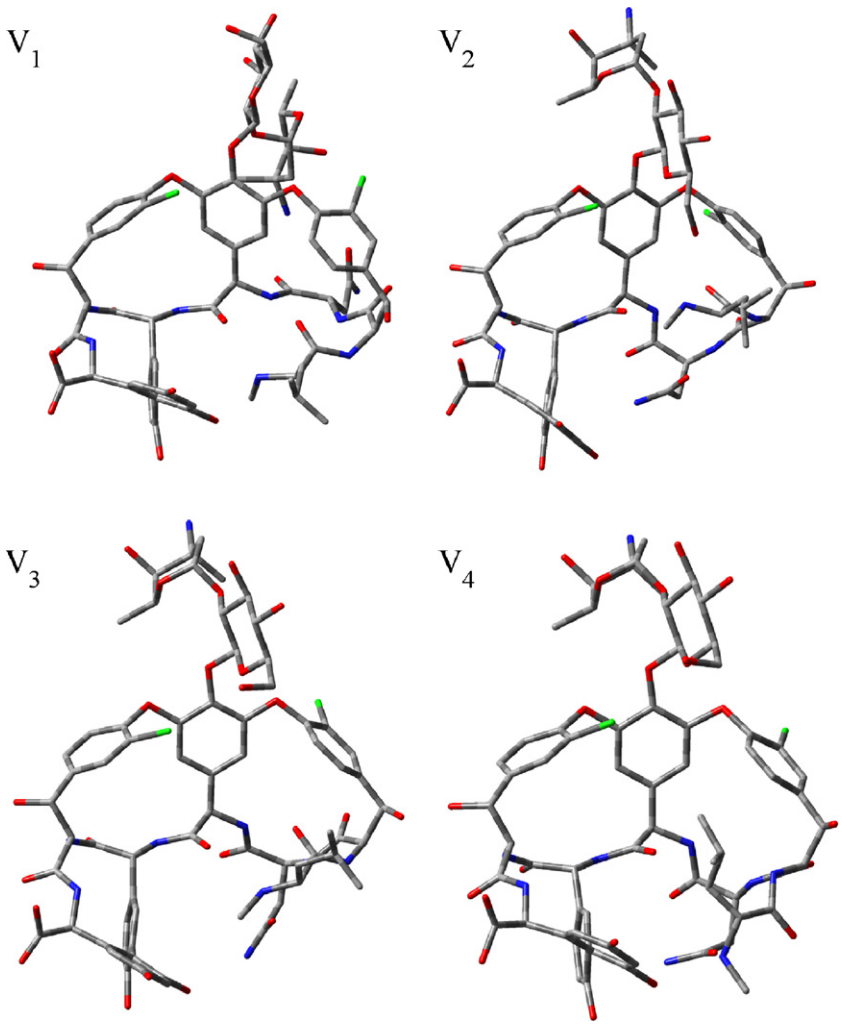

Fig. 4. Optimized ONIOM DFT/B3LYP/6-31g(d):AM1 structures of the four lowest energy conformers of $[V+2H]^{2+}$ obtained from the REMD simulation. Hydrogen atoms are omitted for sake of clarity.

Table 1
Amber 99 potential energies (in kJ/mol) and calculated diffusion cross-section of the six families found by REMD simulations for $[V+2H]^{2+}$. The experimental diffusion cross-section is 318 Å^2 (uncertainty less than 2%).

$[V+2H]^{2+}$	V_1	V_2	V_3	V_4
Amber 99 potential energy (kJ mol^{-1})	0	5	8	32
Calculated diffusion cross-section (Å^2)	321	316	316	313

formers of $[V+2H]^{2+}$ obtained from the REMD simulation leading to an additional conformer V_4. The relative energies of the different conformers are reported in Table 1 and the corresponding structures are depicted in Fig. 4. The overall conformation of vancomycin is similar for all families. The protonated disaccharide moiety does not unfold into the pseudo-peptidic chain of vancomycin, but the H-bonding network involving the charged groups differs from one family to another. The calculated cross-sections for all families (see Table 1) are compatible with ion mobility measurement and we thus cannot exclude any of them. The ONIOM DFT/B3LYP/6-31g(d):AM1 calculated IR spectra of the four families are reported in Fig. 5. The simulated spectrum of conformer V_4 closely agrees with the experiment, with the Amide I and Amide II band shifts being predicted at −10 and −17 cm^{-1}, respectively. This shows a characteristic feature, namely the NH_3^+ group of the disaccharide moiety is not involved in hydrogen bonds. Interestingly, the low-frequency bands (1000–1300 cm^{-1}) are red-shifted for the four conformers. This may indicate that the global scaling factor of the DFT/B3LYP/6-31g(d) level is not appropriate to the present ONIOM DFT/B3LYP/6-31g(d):AM1 level for the modes involved. A more elaborate level of theory could also be required to describe adequately the vibrational modes of the sugar moiety within this frequency range. However, a calculation at the ONIOM DFT/B3LYP/6-31 + g(d):AM1 level for the V_4 family gives a very similar simulated spectrum (see Fig. S3 of the ESI).

The same methodology was applied to the study of the complex involving doubly protonated vancomycin bound to neutral

Table 2
Amber 99 potential energies (in kJ/mol) and calculated diffusion cross-section of the six families of conformers found by REMD simulations for $[V+Ac_2{}^LK^DA^DA+2H]^{2+}$. The experimental diffusion cross-section is 355 Å^2 (uncertainty less than 2%).

$[V+Ac_2{}^LK^DA^DA+2H]^{2+}$	VR_1	VR_2	VR_3	VR_4	VR_5	VR_6
Amber 99 potential energy (kJ mol^{-1})	0	36	37	42	48	55
Calculated diffusion cross-section (Å^2)	376	354	371	362	398	377

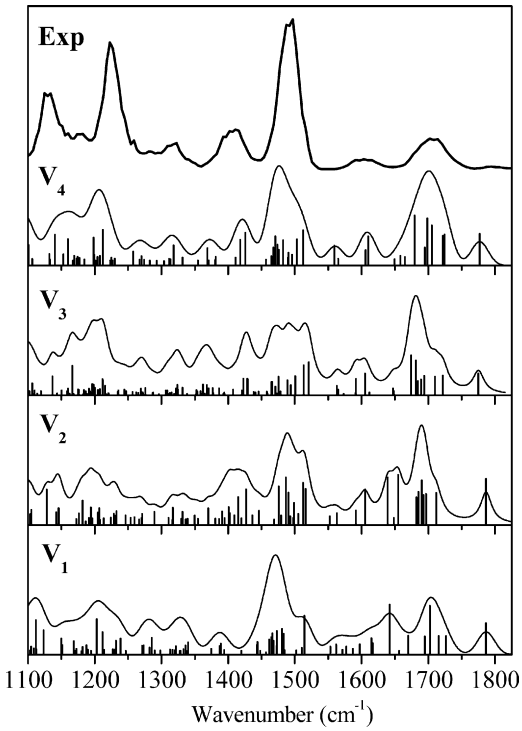

Fig. 5. Comparison between experimental (upper curve) and ONIOM DFT/B3LYP/6-31g(d):AM1 calculated IR spectra of the four conformers of $[V+2H]^{2+}$.

$Ac_2{}^{L}K^{D}A^{D}A$ receptor. A REMD simulation led to several low-lying energy structures in which the receptor explores several binding sites. Clustering of the 120 low-lying conformers revealed the existence of six main families (noted V–R_1 to V–R_6), the protonated disaccharide moiety being the preferred binding site. The calculated diffusion cross-sections for these families are reported in Table 2. While four of them (V–R_1, V–R_3, V–R_5 and V–R_6) cannot account for the most intense mobility peak, the calculated diffusion cross-sections of the V–R_2 and V–R_4 families are in good agreement with the experiment. Their structures are reported in Fig. 6 and the simulated IR spectra are presented in Fig. 7 along with the experimental spectrum. For conformer V–R_2, a relatively fair agreement is found with the IRMPD spectrum, especially for the Amide I and II bands whose positions are predicted at −10 and +15 cm^{-1}, respectively. It is noteworthy that the receptor lies outside and on the other side of the binding pocket of vancomycin. The structure of vancomycin in conformer V–R_2 is slightly modified by the complexation with the receptor as compared to the structure of the bare vancomycin. In particular, its protonated amino $NH_3{}^{+}$ group is involved in H-bonding with the receptor that bends the sugar moiety outside of the vancomycin binding pocket. This last result indirectly points out the importance of the carboxylate moiety (not present in this gas-phase protonated complex) as key receptors for molecular recognition. In addition, the experimental 30 cm^{-1} red-shift of the Amide I band upon complexation is correctly accounted for by the spectra of the V_4 and V–R_2 families. This red-shift is mainly due to strongly bound C=O groups

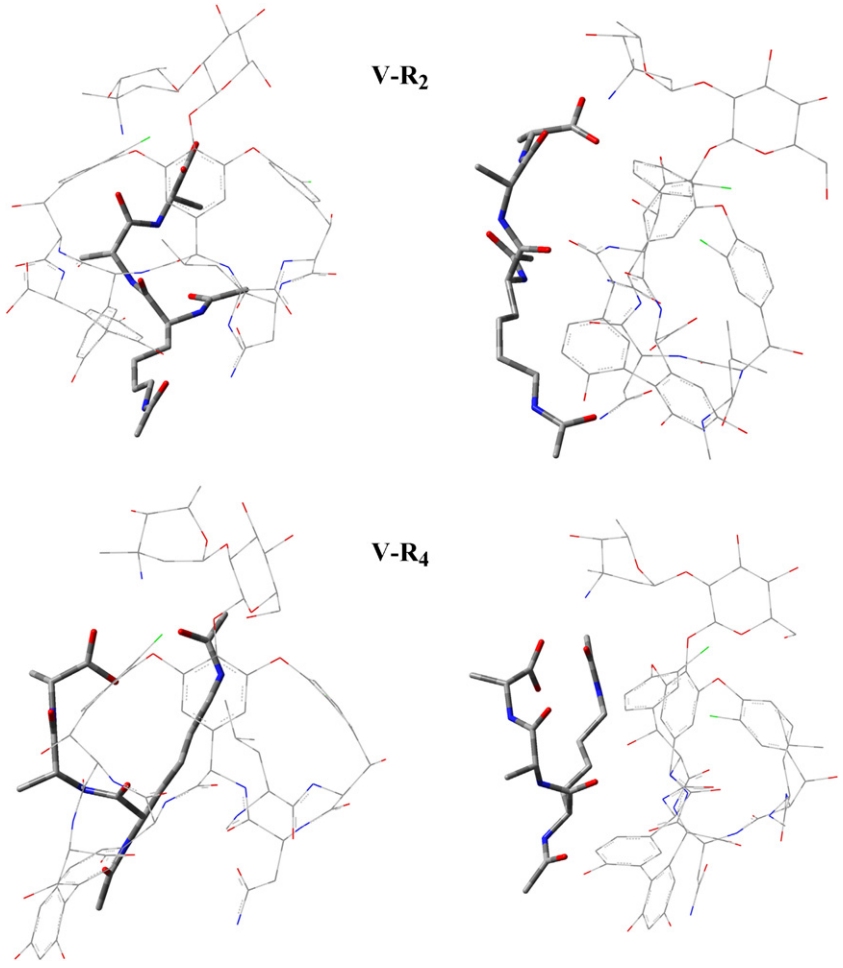

Fig. 6. Optimized ONIOM DFT/B3LYP/6-31g(d):AM1 structures of the two low-energy conformers V–R_2 and V–R_4 of $[V+Ac_2{}^{L}K^{D}A^{D}A+2H]^{2+}$ obtained from the REMD simulation for which the calculated diffusion cross-sections agree with the experiment. Hydrogen atoms are omitted for sake of clarity. Vancomycin is plotted in wireframe, receptor in tube. The receptor is located outside and behind the binding pocket of vancomycin (left, front view; right, side view).

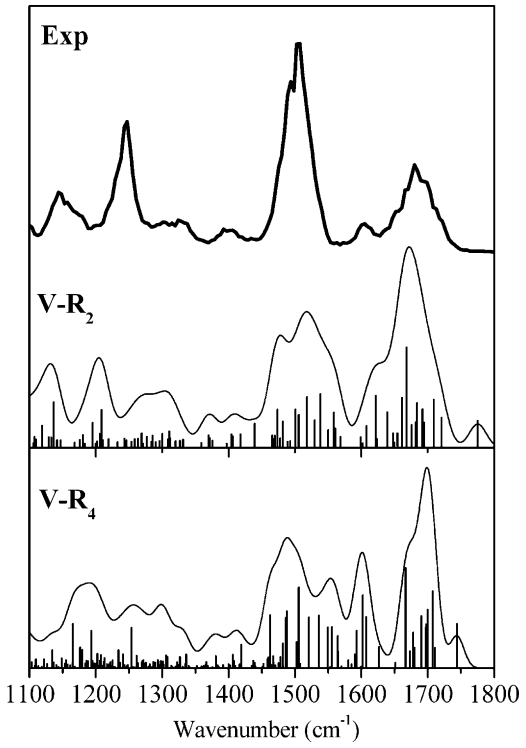

Fig. 7. Comparison between experimental (upper curve) and ONIOM DFT/B3LYP/6-31g(d):AM1 calculated IR spectra of the two conformers of $[V+Ac_2{}^{L}K^{D}A^{D}A+2H]^{2+}$.

of the receptor, in intermolecular H-bonding interaction between the amide and $NH_3{}^{+}$ groups of vancomycin. The blue shift of the Amide II band is also qualitatively reproduced in conformer $V–R_2$ although the width of the calculated band being overestimated. For conformer $V–R_4$, the calculated diffusion cross-section (362 Å^2) is slightly higher than the experiment (355 Å^2), but its simulated IR spectrum is in poor agreement with the experiment. The Amide I band is predicted to be blue-shifted by 20 cm^{-1}, a strong transition at 1550 cm^{-1} is not seen experimentally, and the low-frequency part of the IRMPD spectrum is poorly reproduced. Besides, the full DFT/B3LYP/6-31g(d) single-point energy of this structure optimized at the ONIOM DFT/B3LYP/6-31g(d):AM1 level is 38 kJ/mol higher than the $V–R_2$ family. Interestingly, the $Ac_2{}^{L}K^{D}A^{D}A$ peptide is also bound to the $NH_3{}^{+}$ group, outside the binding pocket.

Recently, Yang et al. carried out SID experiments together with RRKM simulations, and proposed one conformer for $[V+Ac_2{}^{L}K^{D}A^{D}A+2H]^{2+}$ [19]. Its diffusion cross-section turns out to be 370 Å^2 and its simulated IR spectrum is shown in Fig. S4 of the ESI. The spectrum reproduces the main trends seen in the IRMPD experiment, even though a strong band appearing at 1545 cm^{-1} is not seen experimentally. Its cross-section is however too high to be assigned to the main mobility peak but might account for the small shoulder observed around 370 Å^2. This conformer lies 50 kJ/mol above conformer $V–R_2$ at the full DFT/B3LYP/6-31g(d) level (single-point energy after optimization at the ONIOM DFT/B3LYP/6-31g(d):AM1 level).

5. Conclusion

In this paper, we presented the structural investigation of a biological non-covalent complex by means of IR spectroscopy, ion mobility spectrometry and theoretical modeling. We showed that valuable structural information can be obtained from these complementary methods. This combination is well suited to the case of vancomycin and its complexes with the $Ac_2{}^{L}K^{D}A^{D}A$ receptor in positive mode, because their specific native interactions as revealed by X-ray crystallography are lost due to neutralization of the receptor's carboxylate group. The binding site is thus not known *a priori*. The main results of our investigation are as follows. First, the conformational heterogeneity of the gas-phase doubly protonated species is surprisingly low, even for the complex. In particular, only one binding site seems to dominate among the high number found by the conformational sampling. We proposed one main conformer for doubly protonated vancomycin and its complex. In the doubly protonated complex, the receptor is located outside and on the other side of the binding pocket of vancomycin and is involved in hydrogen bonds with the protonated amine group of the disaccharide moiety and two amide bonds of vancomycin. Interestingly, none of the native interactions are preserved in the protonated species.

Acknowledgments

The authors thank the CLIO staff for their technical assistances and the GDR CNRS 2758 for financial support.

Appendix A. Supplementary data

Supplementary data associated with this article can be found, in the online version, at doi:10.1016/j.ijms.2010.05.014.

References

[1] A.N. Chatterjee, H.R. Perkins, Biochemical and Biophysical Research Communications 24 (1966) 489.
[2] D.H. Williams, J.P. Waltho, Biochemical Pharmacology 37 (1988) 133.
[3] J. Liu, K.J. Volk, M.S. Lee, M. Pucci, S. Handwerger, Analytical Chemistry 66 (2002) 2412.
[4] D.H. Williams, Natural Products Reports 13 (1996) 469.
[5] H.R. Perkins, Biochemical Journal 111 (1969) 195.
[6] C.T. Walsh, S.L. Fisher, I.S. Park, M. Prahalad, Z. Wu, Chemistry & Biology 3 (1996) 21.
[7] M. Nieto, H.R. Perkins, Biochemical Journal 123 (1971) 773.
[8] M.P. Williamson, D.H. Williams, Journal of the American Chemical Society 103 (1981) 6580.
[9] P.J. Loll, A.E. Bevivino, B.D. Korty, P.H. Axelsen, Journal of the American Chemical Society 119 (1997) 1516.
[10] Y. Nitanai, T. Kikuchi, K. Kakoi, S. Hanamaki, I. Fujisawa, K. Aoki, Journal of Molecular Biology 385 (2009) 1422.
[11] P.J. Loll, J. Kaplan, B.S. Selinsky, P.H. Axelsen, Journal of Medicinal Chemistry 42 (1999) 4714.
[12] D. Kahne, C. Leimkuhler, W. Lu, C. Walsh, Chemical Review 105 (2005) 425.
[13] T.J.D. Jørgensen, P. Roepstorff, A.J.R. Heck, Analytical Chemistry 70 (1998) 4427.
[14] T.J.D. Jørgensen, D. Delforge, J. Remacle, G. Bojesen, P. Roepstorff, International Journal of Mass Spectrometry 188 (1999) 63.
[15] T.J.D. Jørgensen, P. Hvelplund, J.U. Andersen, P. Roepstorff, International Journal of Mass Spectrometry 219 (2002) 659.
[16] K.F. Haselmann, T.J.D. Jorgensen, B.A. Budnik, F. Jensen, R.A. Zubarev, Rapid Communications in Mass Spectrometry 16 (2002) 2260.
[17] A.J.R. Heck, T.J.D. Jørgensen, M. O'Sullivan, M. von Raumer, P.J. Derrick, Journal of the American Society for Mass Spectrometry 9 (1998) 1255.
[18] Z. Yang, E.R. Vorpagel, J. Laskin, Journal of the American Chemical Society 130 (2008) 13013.
[19] Z. Yang, E.R. Vorpagel, J. Laskin, Chemistry - A European Journal 15 (2009) 2081.
[20] E.G. Robertson, J.P. Simons, Physical Chemistry Chemical Physics 3 (2001) 1.
[21] J. Oomens, B.G. Sartakov, G. Meijer, G. von Helden, International Journal of Mass Spectrometry 254 (2006) 1.
[22] G. Gregoire, M.P. Gaigeot, D.C. Marinica, J. Lemaire, J.P. Schermann, C. Desfrançois, Physical Chemistry Chemical Physics 9 (2007) 3082.
[23] B. Lucas, G. Gregoire, J. Lemaire, P. Maitre, F. Glotin, J.P. Schermann, C. Desfrancois, International Journal of Mass Spectrometry 243 (2005) 105.
[24] N.C. Polfer, J. Oomens, R.C. Dunbar, Physical Chemistry Chemical Physics 8 (2006) 2744.
[25] J. Oomens, J.D. Steill, B. Redlich, Journal of the American Chemical Society 131 (2009) 4310.
[26] M. Seydou, G. Gregoire, J. Liquier, J. Lemaire, F. Lecomte, J.P. Schermann, C. Desfrancois, Journal of the American Chemical Society 130 (2008) 4187.
[27] D. Scuderi, C.F. Correia, O.P. Balaj, G. Ohanessian, J. Lemaire, P. Maitre, ChemPhysChem 10 (2009) 1630.
[28] R. Wu, T.B. McMahon, The Journal of Physical Chemistry B 113 (2009) 8767.
[29] V. Gabelica, F. Rosu, E. De Pauw, J. Lemaire, J.-C. Gillet, J.-C. Poully, F. Lecomte, G. Gregoire, J.-P. Schermann, C. Desfrancois, Journal of the American Chemical Society 130 (2008) 1810.

[30] J. Oomens, N. Polfer, D.T. Moore, L. van der Meer, A.G. Marshall, J.R. Eyler, G. Meijer, G. von Helden, Physical Chemistry Chemical Physics 7 (2005) 1345.
[31] K. Pagel, P. Kupser, F. Bierau, N.C. Polfer, J.D. Steill, J. Oomens, G. Meijer, B. Koksch, G. von Helden, International Journal of Mass Spectrometry 283 (2009) 161.
[32] J.C. Poully, G. Gregoire, J.P. Schermann, Journal of Physical Chemistry A 113 (2009) 8020.
[33] R. Sudha, M.F. Jarrold, Journal of Physical Chemistry B 109 (2005) 11777.
[34] M. Kohtani, T.C. Jones, R. Sudha, M.F. Jarrold, Journal of the American Chemical Society 128 (2006) 7193.
[35] E.S. Baker, S.L. Bernstein, V. Gabelica, E. De Pauw, M.T. Bowers, International Journal of Mass Spectrometry 253 (2006) 225.
[36] E.R. Badman, S. Myung, D.E. Clemmer, Journal of the American Society for Mass Spectrometry 16 (2005) 1493.
[37] B.T. Ruotolo, K. Giles, I. Campuzano, A.M. Sandercock, R.H. Bateman, C.V. Robinson, Science 310 (2005) 1658.
[38] S. Witt, Y.D. Kwon, M. Sharon, K. Felderer, M. Beuttler, C.V. Robinson, W. Baumeister, B.K. Jap, Structure 14 (2006) 1179.
[39] S.L. Koeniger, S.I. Merenbloom, D.E. Clemmer, Journal of Physical Chemistry B 110 (2006) 7017.
[40] M.G. Krone, A. Baumketner, S.L. Bernstein, T. Wyttenbach, N.D. Lazo, D.B. Teplow, M.T. Bowers, J.-E. Shea, Journal of Molecular Biology 381 (2008) 221.
[41] S.L. Bernstein, N.F. Dupuis, N.D. Lazo, T. Wyttenbach, M.M. Condron, G. Bitan, D.B. Teplow, J.-E. Shea, B.T. Ruotolo, C.V. Robinson, M.T. Bowers, Nature Chemistry 1 (2009) 326.
[42] C. Wu, M.M. Murray, S.L. Bernstein, M.M. Condron, G. Bitan, J.-E. Shea, M.T. Bowers, Journal of Molecular Biology 387 (2009) 492.
[43] M.K. Drayss, D. Blunk, J. Oomens, N. Polfer, C. Schmuck, B. Gao, T. Wyttenbach, M.T. Bowers, M. Schafer, International Journal of Mass Spectrometry 281 (2009) 97.
[44] L. Joly, R. Antoine, F. Albrieux, R. Ballivian, M. Broyer, F. Chirot, J. Lemoine, P. Dugourd, C. Greco, R. Mitric, V. Bonacic-Koutecky, Journal of Physical Chemistry B 113 (2009) 11293.
[45] J.C. Poully, F. Lecomte, N. Nieuwjaer, B. Manil, J.P. Schermann, C. Desfrancois, F. Calvo, G. Gregoire, Physical Chemistry Chemical Physics 12 (2010) 3606.
[46] F. Albrieux, F. Calvo, F. Chirot, V. Lepère, Y.O. Tsybin, R. Antoine, J. Lemoine, P. Dugourd, J. Phys. Chem. A (submitted for publication).
[47] L. Mac Aleese, A. Simon, T.B. McMahon, J.M. Ortega, D. Scuderi, J. Lemaire, P. Maitre, International Journal of Mass Spectrometry 249 (2006) 14.
[48] Y. Sugita, Y. Okamoto, Chemical Physics Letters 314 (1999) 141.
[49] D.A. Case, D.A. Pearlman, J.W. Caldwell, T.E. Cheatham III, J. Wang, W.S. Ross, C.L. Simmerling, T.A. Darden, K.M. Merz, R.V. Stanton, A.L. Cheng, J.J. Vincent, M. Crowley, F.V. Tsui, H. Gohlke, R.J. Radmer, Y. Duan, J. Pitera, I. Massova, G.L. Seibel, U.C. Singh, P.K. Weiner, P.A. Kollman, AMBER 7, University of California, San Francisco, CA, 2002.
[50] P.S. Shenkin, D.Q. McDonald, Journal of Computational Chemistry 15 (1994) 899.
[51] M.F. Mesleh, J.M. Hunter, A.A. Shvartsburg, G.C. Schtz, M.F. Jarrold, Journal of Physical Chemistry 100 (1996) 16082.
[52] M.J. Frisch, G.W. Trucks, H.B. Schlegel, G.E. Scuseria, M.A. Robb, J.R. Cheeseman, G. Scalmani, V. Barone, B. Mennucci, G.A. Petersson, H. Nakatsuji, M. Caricato, X. Li, H.P. Hratchian, A.F. Izmaylov, J. Bloino, G. Zheng, J.L. Sonnenberg, M. Hada, M. Ehara, K. Toyota, R. Fukuda, J. Hasegawa, M. Ishida, T. Nakajima, Y. Honda, O. Kitao, H. Nakai, T. Vreven, J. Montgomery, J.A., J.E. Peralta, F. Ogliaro, M. Bearpark, J.J. Heyd, E. Brothers, K.N. Kudin, V.N. Staroverov, R. Kobayashi, J. Normand, K. Raghavachari, A. Rendell, J.C. Burant, S.S. Iyengar, J. Tomasi, M. Cossi, N. Rega, N.J. Millam, M. Klene, J.E. Knox, J.B. Cross, V. Bakken, C. Adamo, J. Jaramillo, R. Gomperts, R.E. Stratmann, O. Yazyev, A.J. Austin, R. Cammi, C. Pomelli, J.W. Ochterski, R.L. Martin, K. Morokuma, V.G. Zakrzewski, G.A. Voth, P. Salvador, J.J. Dannenberg, S. Dapprich, A.D. Daniels, Ö. Farkas, J.B. Foresman, J.V. Ortiz, J. Cioslowski D.J. Fox. *Gaussian 09, Rev A.2*, Wallingford CT, 2009.
[53] NIST and http://cccbdb.nist.gov/vibscalejust.asp.
[54] H.E. Revercomb, E.A. Mason, Analytical Chemistry 47 (1975) 970.
[55] H. Zhang, M. Grabenauer, M.T. Bowers, D.V. Dearden, The Journal of Physical Chemistry A 113 (2009) 1508.